Mast Cell Stabilization: New Mechanism Underlying the Therapeutic Effect of Intense Pulsed Light on Rosacea

Peiyu
the First Affiliated Hospital of Nanjing Medical University
Yunyi Liu
the First Affiliated Hospital of Nanjing Medical University
Jiawen Zhang
Huashan Hospital of Fudan University
Yixuan Liu
the First Affiliated Hospital of Nanjing Medical University
Min Li
the First Affiliated Hospital of Nanjing Medical University
Meng Tao
the First Affiliated Hospital of Nanjing Medical University
Yue Zhang
the First Affiliated Hospital of Nanjing Medical University
Zongxiang Tang
Nanjing University of Chinese Medicine
Wentao Liu
Nanjing Medical University
Yang Xu (yangxu@njmu.edu.cn)
the First Affiliated Hospital of Nanjing Medical University

Research Article

Keywords: Rosacea, intense pulsed light, photobiomodulation, mast cells, degranulation

Posted Date: May 24th, 2022

DOI: https://doi.org/10.21203/rs.3.rs-1665334/v1

Abstract

Background: Rosacea, a chronic inflammatory disorder of the facial skin, is effectively treated by intense pulsed light (IPL).

Objective: To explore the potential molecular mechanism underlying the photobiomodulation effect of IPL for rosacea treatment.

Methods: Skin samples from patients with rosacea were subjected to histological and immunohistological staining. Ten patients were followed up after IPL treatment using the VISIA® skin analysis system, and the severity was assessed. *In vivo*, skin changes in mice with rosacea-like inflammation induced by intradermal injection of 320 μM LL-37 with or without IPL treatment were evaluated using L*a*b colorimetry as well as histological and immunological staining. *In vitro*, LL-37-stimulated mast cells (MCs) with or without IPL treatment were evaluated for protein expression of matrix metalloproteinase (MMP)-9, kallikrein-related peptidase 5 (KLK5), and cathelicidin using western blotting and qRT-PCR.

Results: Profound infiltration of inflammatory cells and evident MC degranulation were found in rosacea skin lesions. The expression of rosacea-related biomarkers and inflammatory cytokines was higher in lesion areas than in non-lesional areas, as demonstrated via immunochemical staining. In all patients, rosacea severity reduced after IPL therapy. *In vivo,* IPL alleviated inflammation in mice with rosacea-like inflammation, as demonstrated by the significantly decreased MMP-9, KLK5, and cathelicidin expression and reduced percentage of degranulating MCs. *In vitro*, IPL decreased MMP-9, KLK5, and cathelicidin expression in P815 cells, reducing the release of inflammatory cytokines and inhibiting rosacea-like inflammatory reactions.

Conclusion: The photobiomodulation effect of IPL for rosacea treatment may inhibit MC degranulation and alleviate inflammatory reactions.

1. Introduction

Rosacea is a chronic and recurrent inflammatory skin disease mainly characterized by flushing, telangiectasia, papules, and pustules[1]. According to the 2002 National Rosacea Society (NRS), rosacea lesions are typically classified into four main subtypes based on their morphological appearance[2]. However, an updated 2017 guideline emphasizes a more patient-centered approach to the phenotype[3]. The pooled proportion of individuals with rosacea in the 32 studies of the latest international population epidemiological meta-analysis was 5.46%[4]. Although the pathogenesis of rosacea is still unclear, innate immune dysregulation, commensal microbiota imbalance, and neurovascular abnormalities may contribute to higher levels of KLK5 protease in the skin of patients with rosacea than in healthy individuals[1]. Additionally, studies have shown that the active form of the antimicrobial peptide cathelicidin, LL-37, triggers the development of rosacea[5]. Our previous study showed that rosacea treatment using carvedilol is also related to the inhibition of Toll-like receptor 2 (TLR2) activation[6].

Mast cells (MCs) play a key role in the pathogenesis of rosacea[7]. LL-37 could activate Mas-related gene X2 (MrgX2) on MCs to trigger degranulation, leading to an inflammatory response. MCs are involved in innate immunity and neurogenic inflammation. When peripheral nerve endings approach the early stage, sensory nerve-derived neuropeptides can activate MCs and promote the release of inflammatory factors, which mediates neurogenic inflammation[8]. MCs are a common bridge involved in innate immune abnormalities, neurovascular imbalance, and neurogenic inflammation. Therefore, the molecular mechanisms underlying the role of MCs in the pathogenesis of rosacea may be an important research focus.

Intense pulse light (IPL) is a new photo-based therapy for skin diseases, including rosacea, as mentioned in several guidelines and consensuses[9–11]. IPL could effectively alleviate erythema telangiectasia and papule pustule in patients with rosacea[12–14]. IPL is a broadband of light that can provide spectra with different wavelength combinations between 500 and 1200 nm using different filters[15]. It is an incoherent light source with variable pulses, durations, and intervals. IPL effectively treats paroxysmal flushing, erythema pilaris, and vasodilatation[13, 16, 17]. The effect of IPL on rosacea may be related to selective photothermal effects and photobiomodulation[18–21]. Selective photothermal effects include targeting hemoglobin to destroy dilated blood vessels[11], reducing sebum secretion[22], and killing demodex[23]. Selective photothermal action is the principal theoretical basis of phototherapy; however, the photobiomodulation effect remains unclear, especially the effect of low-density IPL on rosacea. Recently, Lee et al. reported that light-emitting diodes (LED) could alleviate the severity of rosacea by downregulating TLR2, KLK5, and cathelicidin expression[24]. Taylor et al. found that IPL could also treat acne by downregulating tumor necrosis factor (TNF) -α expression[25]. Therefore, the anti-inflammatory photobiomodulatory effect of IPL deserves further study.

MCs originate from bone marrow CD34 + progenitor cells[26]. Activated MCs can promote the release of different mediators, such as histamine, proteases (tryptase, chymase, and MMP-9), and a series of cytokines (IL-1, IL-8, and TNF-α). Histamine can cause vasodilation and itching, and tryptase can induce chemotactic fibroblasts[27]; together with MMPs, these participate in the development of rosacea. Activated MCs also secrete cathelicidin. These mediators further amplify skin inflammation and angiogenesis, thereby promoting progression[7]. Chymase and MMP-9 are essential markers for the presence and activation of MCs in rosacea skin[7]. MMPs can also activate KLK5, and MMP-9 produces more active LL-37 by activating the KLK5 proenzyme to activate KLK5[8]. Doxycycline can exert a therapeutic effect by directly inhibiting MMP activity[28].

In our clinical practice, low-fluence IPL (11 J/cm^2, 590 nm filter, single pulse, pulse width of 20 ms, two passes) exhibited good clinical effects on rosacea. However, whether the photobiomodulation effect of IPL on rosacea is related to MCs requires further study.

2. Materials And Methods

2.1. Clinical Observation of Rosacea Patients Treated With IPL

All 10 patients were treated with a Lumenis M22® (Lumenis Ltd., Israel) xenon-based IPL device, using a 590 nm filter with a sapphire-cooled 15 × 35 mm² cylindrical light guide (with a fluence of 11 J/cm^2, single pulse, and pulse duration of 20 ms, two passes). Before and 1 month after initial IPL therapy, the severity of rosacea was evaluated by two independent senior dermatologists using the clinician's erythema assessment (CEA) and investigator global assessment (IGA), two 5-point grading scales[7, 29]. Facial images were obtained and analyzed using the VISIA®6.0 complexion analysis system (Canfield Scientific Inc., Parsippany, NJ, USA). The facial images were saved, the red area was processed by ImageJ, and the percentage of erythema area was calculated and further analyzed using GraphPad Prism 6.

2.2. Animals

Twenty-eight female BALB/c mice (6–8 weeks old, weighing 18–22 g) were purchased from Puer BHQ Laboratory Animals, Inc. (certification no: SCXK HU 2018-0006; Shanghai, China). Five mice were housed per cage under pathogen-free conditions with soft bedding under controlled temperature (22 ± 2 ℃) and a 12 h light/dark cycle (lights on at 8:00 a.m.). Mice were acclimatized to the testing environment for 2 days before starting the experiments. All mice were matched for age and body weight in each experimental group.

2.3. Rosacea-like Inflammation Mouse Model

A well-established model was used based on the previous studies[5, 30]. Female BALB/c mice were shaved 24 h prior to the experiment. LL-37 (amino acid sequence: LLGDFFRKSKEKIGKEFKRIVQRIKDFLRNLVPRTE[6]) was synthesized by Sangon Biological Technology (Shanghai, China) at > 99% purity and was dissolved (320 μM) in phosphate-buffered saline (PBS) in advance and stored at 4 ℃ for further use. After weighing, mice were anesthetized through intraperitoneal injection of pentobarbital sodium (50 mg/kg), and then LL-37 (320 μM in PBS) was intradermally injected into a pre-drawn circle on the back to form a picumulus. Subsequently, the mice were returned to the animal room for regular feeding.

BALB/c mice were randomly divided into four groups (seven mice per group): control (PBS, 50 μL, i.d.), LL-37 (LL-37, 320 μM, 50 μL, i.d.), LL-37 + IPL (320 μM LL-37, 50 μL, i.d.+IPL treatment), and IPL group (PBS, 50 μL, i.d.+IPL treatment). For IPL therapy, the same Lumenis M22® device was used (with a fluence of 11 J/cm^2, single pulse, and pulse duration of 20 ms) for a single pass on the treated sites of the mice at 12 h after the last injection.

For the LL-37 group, injections were administered four times every 12 h consecutively, while the control group was administered 50 μL PBS. IPL treatment was performed in the LL-37 + IPL and IPL groups 12 h after the last injection. The light guide was kept in contact with the treated sites during the treatment.

Mice were photographed 1 h after the IPL irradiation. Erythema severity was assessed and quantified as a^* value using an L^*a^*b colorimeter (CR-10 plus, Konica Minolta, Japan).

At 72 h after the last injection, samples of skin lesions were collected for further analysis.

2.4. Histopathologic Analysis of Human and Mouse Skin Samples

Mouse skin samples were fixed overnight in 4% buffered formalin for 24 h, embedded in paraffin, sliced into 4-mm sections, and stained with hematoxylin and eosin (H&E) or toluidine blue. Images were captured using an optical microscope (Leica, Germany) at 200× and 400× magnifications by a blinded observer. Degranulation of MCs was considered if four or more extruded granules could be seen neighboring a cell or the cell outline was disrupted. Conversely, intact cells demonstrated deep blue staining[30, 31].

2.5. Immunohistochemical Analysis of Human and Mouse Skin Samples

Paraffin sections of tissue were washed with PBS, dewaxed, treated with 3% H_2O_2 for 10 min, repaired with citrate buffer, blocked with serum, and then incubated with different antibodies. The antibodies against MMP-9 (R&D, Santa Clara, CA, USA; 2.0 mg/mL, diluted by 1:100), human-KLK5 (Abcam, Waltham, MA, USA; 1.295 mg/mL, diluted by 1:100), human-Cathelicidin (Abcam; 3.44 mg/mL, 1:150), human-IL-6 (Santa Cruz, USA; 200 μg/mL, diluted by 1:100), mouse-Cathelicidin (Biorbyt, St Louis, MO, USA; 1 mg/mL, 1:200), mouse-IL-6 (Santa Cruz, USA, 200 μg/mL, 1:200), TNF-α (Abcam; 0.2 mg/mL, 1:100), and IL-1β (Abcam; 2 mg/mL, 1:100), MC Tryptase (Hua Bio, China; 1 mg/mL, 1:150), Histamine (Novus biological, Englewood, CO, USA, 15 mmol/mL, 1:150) were incubated for 1 h at room temperature. Negative controls were incubated with the diluent instead of the primary antibody. The slides were incubated with HRP-labeled secondary antibody for 30 min, treated with diaminobenzidine, and counterstained with hematoxylin. Subsequently, the slides were differentiated, dehydrated, cleared, covered with neutral resin, and observed and imaged using a microscope (Leica, Germany) at 200× magnification. Light to dark brown staining indicates positive results. Immunohistochemical (IHC) staining was semi-quantitatively analyzed and assigned using ImageJ (v1.51, https://imagej.nih.gov/).

2.6. Immunofluorescent Examination of Mouse Skin Samples

The paraffin sections of mouse skin were washed, dewaxed, treated with 3% H_2O_2, repaired using antigen, blocked using donkey serum containing 0.3% TritonX-100 for 2 h at room temperature, and treated with primary antibodies including MMP-9, KLK5 at 4°C overnight. Next, the slices were incubated with the secondary antibody (Jackson, Louisiana, NO, USA; 15 mg/mL, 1:300) for 2 h at 37°C, and sections were subsequently washed and counterstained with DAPI for 10 min. Images were captured using a fluorescence microscope at 100× magnification (Leica, Germany).

2.7. Cell Culture and Grouping

The mouse MC tumor P815 cell line (RRID: CVCL_2154, ATCC TIB-64; American Type Culture Collection, Manassas, VA, USA) were provided by Nanjing University of Chinese Medicine and were cultured in RPMI-1640 medium (Gibco, Waltham, MA, USA) supplemented with 10% fetal bovine serum (Gibco), 1% penicillin-streptomycin (Gibco) in a cell incubator, which was set at 5% CO_2 at 37°C. The cells were equalized into Petri dishes (35 mm × 10 mm) and then stimulated using LL-37 (2.0 μM) for 6 h with or without IPL treatment (single pulse, 11 J/cm^2 with a 20 ms pulse duration) immediately after LL-37 administration. Proteins and RNA were then extracted. Before treatment, the supernatant was discarded, and the cells were rinsed twice with PBS and then replaced with fresh RPMI-1640 medium (phenol red-free, serum-free) to exclude the influence of light. The levels of related proteins and RNAs were detected.

2.8. Cell Viability Assay

P815 cells were seeded in 96-well plates and processed for 6 h. CCK8 solution (supernatant; Yi Sheng Biotechnology, China) was added at 10 μL per well. After a 3-h incubation, the optical density (OD) at 450 nm was measured using a microplate reader (Thermo Fisher, Waltham, MA, USA).

2.9. Western Blot

Samples, including skin tissue segments, were collected, lysed in RIPA lysate with 1% protease and phosphatase inhibitor. Proteins were extracted using methanol and chloroform and quantified using the BCA Protein Assay (Thermo Fisher). Equivalent amounts of proteins (animal proteins, 30 μg; cell proteins, 10 μL) were loaded and separated by SDS-PAGE. MMP-9, and KLK5, cathelicidin, and GAPDH were detected using 8% and 10% SDS-PAGE gels, respectively. All proteins were transferred onto polyvinylidene fluoride membranes (Millipore, Burlington, MA, USA) and blocked for 2 h at room temperature. Ponceau S (Sangon Biological Technology, China) was used to stain and detect the total proteins in cell supernatant before being blocked. The membranes were then probed with primary antibodies overnight at 4°C. The dilutions of the antibodies against GAPDH (Santa Cruz; 100 μg/mL, 1:800), MMP-9 (Proteintech, Rosemont, IL, USA; 400 μg/mL, 1:1000), KLK5 (Abcam; 1 mg/mL, 1:1000), cathelicidin (Abcam; 3.89 mg/mL, 1:1000). Finally, the membranes were incubated with the corresponding secondary antibodies (Sigma, Burlington, MA, USA, 1:5000). The bands were developed using an enhanced chemiluminescence reagent (Beyotime, China). Data were obtained using the Molecular Imager and analyzed using ImageJ software (NIH, USA).

2.10. Quantitative Real-Time Polymerase Chain Reaction (qRT-PCR)

Total RNA was extracted from the mouse skin tissue and P815 cells using TRIzol reagent (Invitrogen, Waltham, MA, USA). According to standard protocols, 500 ng RNA was reverse-transcribed into 10 μL cDNA using HiScript® RT SuperMix (Vazyme, China). qRT-PCR was performed with SYBR Green Master Mix (Vazyme, China) in the QuantStudio 5 Real-Time PCR Detection System (Thermo Fisher). Relative expression levels were calculated using the $2^{-\Delta\Delta Ct}$ method after normalization with GAPDH. We used the

formulas $\Delta Ct = Ct_{gene} - Ct_{GAPDH}$ and $\Delta\Delta Ct = \Delta Ct -$ mean value of ΔCt in the control group; all primers used are listed in **Table S3**.

2.11 Enzyme-Linked Immunosorbent Assay (ELISA)

ELISA reagent kits (Yi Fei Xue Biotechnology, China) for histamine, β-Hex, TNF-α, IL-8, and IL-1β were used following the manufacturer's protocols. Sample addition, incubation, washing, and developing were performed in sequence, and the OD of each well was measured at 450 nm.

2.12 Statistical Analysis

GraphPad Prism 6 (LaJolla, CA, USA) was used to conduct all statistical analyses. Student's t-test was used to evaluate the differences between the two groups. Results between more than two groups were compared using one-way ANOVA. Data are presented as the mean ± SEM of independent experiments. All statistical tests described as significant were based on a criterion of $P < 0.05$.

3. Results

3.1. Profound Infiltration of Inflammatory Cells and Activation of MCs

Under the microscope, based on H&E-stained sections, profound infiltration of inflammatory cells in the lesional area of rosacea was found compared with the surrounding non-lesional area **(Figure S1a)**. Furthermore, toluidine blue staining revealed degranulated MCs and granules in the skin lesion area **(Figure S1b)**. Additionally, the expression of MMP-9, KLK5, LL-37, cathelicidin, TNF-α, IL-1β, and IL-6 in the skin lesion area was enhanced compared to that in the surrounding area, as revealed by immunohistochemical staining **(Figure S1c–h)**. This indicated that MCs were abnormally activated, and related enzymes, including MMP-9 and KLK5, were involved in LL-37 processing and increased levels of cathelicidin and pro-inflammatory factors in rosacea.

3.2. Low-Fluence IPL was Effective for Facial Erythema in Patients with Rosacea

At the 1-month follow-up, evident alleviation of clinical symptoms of the two patients with rosacea was found **(Fig. 1a–d)**, showing a significant difference in erythema index determined by ImageJ, IGA, and CEA score (**Fig. 1e–g**, respectively). Additionally, no evident adverse reactions were reported by either patient.

3.3. IPL Inhibits MC degranulation in the Rosacea-Like Inflammation Induced by LL-37 in Mice

We evaluated the effect of IPL on LL-37 induced inflammation in mice according to the protocol shown in **Fig. 2a**. Inflammation was observed in mice in the LL-37 group, while IPL significantly attenuated the inflammation reaction induced by LL-37 **(Fig. 2b–e)**. IPL decreased redness scores **(Fig. 2n)**; the average redness score showed an increasing tendency in the LL-37 group and a decreased tendency from 10.9–9.0 in the LL-37 + IPL group. In skin histopathology in mice, H&E staining of the murine tissue of the back skin showed hyperkeratosis and increased infiltration of inflammatory cells in the LL-37 group **(Fig. 2f–g)**. Simultaneously, IPL treatment notably reduced the epidermal thickness and infiltration of inflammatory cells **(Fig. 2h)**. Toluidine blue staining was used to observe MC infiltration and count the number of MCs in 10 random fields of view under an optical microscope. IPL markedly ameliorated the infiltration and degranulation of MCs at 400× magnification **(Fig. 2j–m)**. Eventually, the numbers and degranulation percentage of MCs were analyzed using GraphPad Prism 6 **(Fig. 2o–p)**. Altogether, these results suggest that IPL treatment could ameliorate LL-37-induced rosacea-like inflammation, while IPL treatment alone did not cause significant changes.

The expression of MC-related proteases, including MMP-9, histamine, and tryptase, was visualized using immunochemical staining. The results illustrated that proteases were significantly secreted in the LL37-induced rosacea-like mouse model but subsided after IPL treatment **(Fig. 3a)**. KLK5 and cathelicidin, reliable biomarkers for rosacea, showed a similar tendency **(Fig. 3a)**. Cytokine IL-6 immunochemical staining revealed the level of inflammatory expression among the groups **(Fig. 3a)**. The results were processed using ImageJ to show statistical significance **(Fig. 3b–g)**.

Western blotting showed that IPL treatment significantly reduced LL37-induced MMP-9, KLK5, and cathelicidin expression **(Fig. 4a–c)**. The same result was observed in fluorescence intensity during immunofluorescence staining of MMP-9 and KLK5 **(Fig. 5a-b)**. Furthermore, ELISA data showed that the expression of histamine and β-Hex, essential markers of MC presence and activation, increased in the LL-37 group and decreased in the LL-37 + IPL group. The pro-inflammatory factors TNF-α and IL-8 showed a similar tendency **(Fig. 4d)**. qRT-PCR also revealed that the LL-37 group had significantly upregulated *Camp, Mmp9, Klk5, Cma1, Tpsab1, Cxcl2, Il1b, Il6*, and *Tnfa* expression compared with that in the control group, while it was significantly downregulated in the LL-37 + IPL group **(Fig. 4e)**.

3.4. IPL Inhibits LL-37-Induced Degranulation of MCs and Inflammation in P815 Cells

The cell viability assay demonstrated that the 2.5 μM LL-37 concentration had a significantly negative effect on the viability of P815 cells, and we chose 2.0 μM LL-37 as a stimulant in the cell experiment **(Fig. 6b)**. IPL irradiation doses ≥ 17 J/cm^2 had a significant positive effect on the viability of MCs **(Fig. 6a)**. Combining the light doses for animals and humans, we chose 11 J/cm^2 as the treatment dose without affecting viability. The western blot results showed that IPL treatment reduced MMP-9, KLK5, and cathelicidin expression in P815 cells induced by LL-37 **(Fig. 6c–f)**. In contrast, IPL treatment ameliorated LL37-induced histamine and β-Hex expression in P815 cells **(Fig. 6g)**. We also examined the supernatant from P815 cells and found that the secretion of TNF-α, IL-6, and IL-8 increased in the LL-37 group and

decreased in the LL-37 + IPL group **(Fig. 6g)**. Additionally, we detected that the expression of genes related to *Cma1, Tpsab1, Tnfa, Il6*, and *Il8* was consistent with the protein expression levels **(Fig. 6h)**.

4. Discussion

Studies have suggested an association between MCs and pathogenesis of rosacea and have shown that the number and activity of MCs are higher in lesional skin than in non-lesional skin of patients with rosacea[7, 32]. The histological results of our study are consistent with this, showing increased MC infiltration and expression of related enzymes in the lesion areas.

IPL was commercialized in 1994 as a medical device for the treatment of vascular lesions owing to its selective photothermal action, and the range of potential indications has continued to expand with subsequent device updates. By selectively targeting melanin, hemoglobin, and water as the primary chromophores, IPL provides an effective approach for treating skin pigmentation and vascular disease as well as for skin rejuvenation. In addition to the photothermal effect, photobiomodulation, where visible and infrared light induces intracellular changes at the gene and protein levels, is also an important therapeutic mechanism. Siqueira et al. found that LEDs could exert therapeutic effects in an ovalbumin-induced mouse asthma model by inhibiting MC activation and degranulation[33]. Additionally, Kouhkheil et al. found that photons could effectively accelerated wound healing by inhibiting the degranulation of MCs in diabetic rats[34]. This provides a new direction for the IPL treatment of rosacea. Whether MCs are involved in the process of IPL treatment of rosacea warrants further research.

Our preliminary screening results suggested that yellow light (590 nm filter) had better outcomes than red light (640 nm filter), even with similar parameters **(Figure S2)**. Therefore, we used yellow light in our study. In this study, we demonstrated that IPL could alleviate rosacea-like inflammation by inhibiting MC activation *in vitro* and *in vivo*. To the best of our knowledge, this is the first study to elucidate the anti-inflammatory mechanism of IPL in rosacea treatment. In clinical treatment, we found that the use of 11 J/cm^2 of IPL did not cause facial burning but effectively relieved rosacea symptoms. During the clinical follow-up, the clinical symptoms of patients with rosacea were significantly alleviated after a single IPL (590 nm filter, single pulse, pulse width 20 ms, two passes), and the VISIA® analysis showed a decreased proportion of facial erythema and decreased clinical scores. Additionally, we found an increase in the infiltration and activation of MCs in skin lesions of patients with rosacea compared with that in surrounding non-lesional areas, increased levels of related biological markers MMP-9, KLK5, and cathelicidin, as well as increased levels of inflammatory factors, indicating that MCs are involved in inflammation. Similar results were also found in the rosacea-like mouse model, in which levels of rosacea MC-related enzymes and biological markers were significantly increased in the model mice, but after IPL treatment, the indexes tended to decrease. Additionally, western blotting and qRT-PCR showed that the expression of related indicators and genes increased in the rosacea-like mouse model but significantly decreased in the IPL-treated group. *In vitro*, P815 cell experiments confirmed that IPL treatment could reduce the secretion of MMP-9, KLK5, and cathelicidin and reduce inflammation by inhibiting LL-37-induced MC activation. In summary, low-energy IPL (590 nm filter) can treat rosacea by inhibiting MC

degranulation, thus inhibiting downstream inflammatory responses, suggesting that light is also a good MC membrane stabilizer.

Our study has some limitations. Besides the collection of clinical data before and after IPL treatment in patients with rosacea, there was no direct evidence of related histopathological changes. Additionally, rosacea is a facial disease, and skin tissue removal will lead to local scarring; furthermore, there is still some difficulty in performing two skin biopsies on the face. Finally, whether other wavelengths of light have similar effects requires further research.

5. Conclusion

Low-energy IPL of a specific wavelength can stabilize MC membranes, inhibit MC activation, and alleviate the inflammatory response, thereby facilitating rosacea treatment.

Declarations

Funding

This work was supported by the Chinese National Natural Science Foundation (81301384).

Conflicts of interests

The authors declare no conflict of interest.

Availability of data and material

All data included in this study are available upon request by contact with the corresponding author.

Authors' contributions

PYJ, **JWZ** and **YXL** designed and supervised the study**. PYJ**, **YYL** and **JWZ** completed the majority of experiment and and wrote the first draft. **ML**, **MT**, **YZ** and **ZXT** performed material preparation, data collection and analysis. **YX** and **WTL** reviewed and edited the first draft of the manuscript. All authors reviewed the manuscript.

Ethics approval

All patients provided written informed consent, and the study was approved by the Ethics Committee of the First Affiliated Hospital of Nanjing Medical University (2020-SRFA-082).

Mouse care and treatment protocols were approved by Nanjing Medical University Animal Care and Use Committee (Nanjing, Jiangsu, China).

Consent to participate

Informed consent was obtained from all individual participants included in the study.

Consent for publication

The authors affirm that human research participants provided informed consent for publication of the images in **Figure 1a–d**.

Acknowledgements

Thanks for the participating investigators, patients, as well as colleagues involved in the conduct of the study. Funding for this study was provided by Chinese National Natural Science Foundation (81301384).

References

1. A.M. Two, W. Wu, R.L. Gallo, T.R. Hata, Rosacea, J. Am. Acad. Dermatol. 72 (5) (2015) 749-758, https://doi.org/10.1016/j.jaad.2014.08.028.
2. F. Anzengruber, J. Czernielewski, C. Conrad, L. Feldmeyer, N. Yawalkar, P. Häusermann, A. Cozzio, C. Mainetti, D. Goldblum, S. Läuchli, L. Imhof, C. Brand, E. Laffitte, A.A. Navarini, Swiss S1 guideline for the treatment of rosacea, J Eur Acad Dermatol Venereol 31 (11) (2017) 1775-1791, https://doi.org/10.1111/jdv.14349.
3. R.L. Gallo, R.D. Granstein, S. Kang, M. Mannis, M. Steinhoff, J. Tan, D. Thiboutot, Standard classification and pathophysiology of rosacea: The 2017 update by the National Rosacea Society Expert Committee, J. Am. Acad. Dermatol. 78 (1) (2018) 148-155, https://doi.org/10.1016/j.jaad.2017.08.037.
4. L. Gether, L.K. Overgaard, A. Egeberg, J.P. Thyssen, Incidence and prevalence of rosacea: A systematic review and meta-analysis, Br J Dermatol 179 (2) (2018) 282-289, https://doi.org/10.1111/bjd.16481.
5. K. Yamasaki, A. Di Nardo, A. Bardan, M. Murakami, T. Ohtake, A. Coda, R.A. Dorschner, C. Bonnart, P. Descargues, A. Hovnanian, V.B. Morhenn, R.L. Gallo, Increased serine protease activity and cathelicidin promotes skin inflammation in rosacea, Nat. Med. 13 (8) (2007) 975-980, https://doi.org/10.1038/nm1616.
6. J. Zhang, P. Jiang, L. Sheng, Y. Liu, Y. Liu, M. Li, M. Tao, L. Hu, X. Wang, Y. Yang, Y. Xu, W. Liu, A novel mechanism of carvedilol efficacy for rosacea treatment: Toll-Like receptor 2 inhibition in macrophages, Front Immunol 12 (2021) 609615, https://doi.org/10.3389/fimmu.2021.609615.
7. Y. Muto, Z. Wang, M. Vanderberghe, A. Two, R.L. Gallo, A. Di Nardo, Mast cells are key mediators of cathelicidin-initiated skin inflammation in rosacea, J. Invest. Dermatol. 134 (11) (2014) 2728-2736, https://doi.org/10.1038/jid.2014.222.
8. V.D. Schwab, M. Sulk, S. Seeliger, P. Nowak, J. Aubert, C. Mess, M. Rivier, I. Carlavan, P. Rossio, D. Metze, J. Buddenkotte, F. Cevikbas, J.J. Voegel, M. Steinhoff, Neurovascular and neuroimmune

aspects in the pathophysiology of rosacea, J Investig Dermatol Symp Proc 15 (1) (2011) 53-62, https://doi.org/10.1038/jidsymp.2011.6.

9. F. Anzengruber, J. Czernielewski, C. Conrad, L. Feldmeyer, N. Yawalkar, P. Hausermann, A. Cozzio, C. Mainetti, D. Goldblum, S. Lauchli, L. Imhof, C. Brand, E. Laffitte, A.A. Navarini, Swiss S1 guideline for the treatment of rosacea, J Eur Acad Dermatol Venereol 31 (11) (2017) 1775-1791, https://doi.org/10.1111/jdv.14349.
10. D. Thiboutot, R. Anderson, F. Cook-Bolden, Z. Draelos, R.L. Gallo, R.D. Granstein, S. Kang, M. Macsai, L.S. Gold, J. Tan, Standard management options for rosacea: The 2019 update by the National Rosacea Society Expert Committee, J. Am. Acad. Dermatol. 82 (6) (2020) 1501-1510, https://doi.org/10.1016/j.jaad.2020.01.077.
11. E. Tanghetti, R.J. Del, D. Thiboutot, R. Gallo, G. Webster, L.F. Eichenfield, L. Stein-Gold, D. Berson, A. Zaenglein, Consensus recommendations from the American acne & rosacea society on the management of rosacea, part 4: A status report on physical modalities and devices, Cutis 93 (2) (2014) 71-76.
12. R. Kassir, A. Kolluru, M. Kassir, Intense pulsed light for the treatment of Rosacea and Telangiectasias, J. Cosmet. Laser Ther. 13 (5) (2011) 216-222, https://doi.org/10.3109/14764172.2011.613480.
13. P. Papageorgiou, W. Clayton, S. Norwood, S. Chopra, M. Rustin, Treatment of rosacea with intense pulsed light: Significant improvement and long-lasting results, Br J Dermatol 159 (3) (2008) 628-632, https://doi.org/10.1111/j.1365-2133.2008.08702.x.
14. Y. Zhang, S. Jiang, Y. Lu, W. Yan, H. Yan, Y. Xu, T. Xu, Y. Li, L. Geng, X. Gao, H. Chen, A decade retrospective study of light/laser devices in treating nasal rosacea, The Journal of dermatological treatment 31 (1) (2020) 84-90, https://doi.org/10.1080/09546634.2019.1580669.
15. M.A. Hofmann, P. Lehmann, Physical modalities for the treatment of rosacea, J. Dtsch. Dermatol. Ges. 14 Suppl 6 (2016) 38-43, https://doi.org/10.1111/ddg.13144.
16. S. A, K. G, K. M, G. H, G. A, G. S, G. M, Rosacea management: A comprehensive review., J Cosmet Dermatol (2022), https://doi.org/10.1111/jocd.14816.
17. K.A. Mark, R.M. Sparacio, A. Voigt, K. Marenus, D.S. Sarnoff, Objective and quantitative improvement of rosacea-associated erythema after intense pulsed light treatment, Dermatol. Surg. 29 (6) (2003) 600-604, https://doi.org/10.1046/j.1524-4725.2003.29141.x.
18. H. Serrage, V. Heiskanen, W.M. Palin, P.R. Cooper, M.R. Milward, M. Hadis, M.R. Hamblin, Under the spotlight: Mechanisms of photobiomodulation concentrating on blue and green light, Photochem Photobiol Sci 18 (8) (2019) 1877-1909, https://doi.org/10.1039/c9pp00089e.
19. M. R Hamblin, Mechanisms and applications of the anti-inflammatory effects of photobiomodulation, AIMS Biophysics 4 (3) (2017) 337-361, https://doi.org/10.3934/biophy.2017.3.337.
20. H. Husein-Elahmed, M. Steinhoff, Light-based therapies in the management of rosacea: A systematic review with meta-analysis, Int. J. Dermatol. (2021), https://doi.org/10.1111/ijd.15680.

21. S.J. Dell, Intense pulsed light for evaporative dry eye disease, Clin Ophthalmol 11 (20) (2017) 1167-1173, https://doi.org/10.2147/OPTH.S139894.
22. J. Zdrada, A. Stolecka-Warzecha, W. Odrzywolek, A. Deda, B. Blonska-Fajfrowska, S. Wilczynski, Impact of IPL treatments on parameters of acne skin, J Cosmet Dermatol Feb 1 (2022) online, https://doi.org/10.1111/jocd.14802.
23. H.A. Fishman, L.M. Periman, A.A. Shah, Real-Time video microscopy of in vitro demodex death by intense pulsed light, Photobiomodul Photomed Laser Surg 38 (8) (2020) 472-476, https://doi.org/10.1089/photob.2019.4737.
24. J.B. Lee, S.H. Bae, K.R. Moon, E.Y. Na, S.J. Yun, S.C. Lee, Light-emitting diodes downregulate cathelicidin, kallikrein and toll-like receptor 2 expressions in keratinocytes and rosacea-like mouse skin, Exp. Dermatol. 25 (12) (2016) 956-961, https://doi.org/10.1111/exd.13133.
25. M. Taylor, R. Porter, M. Gonzalez, Intense pulsed light may improve inflammatory acne through TNF-alpha down-regulation, J. Cosmet. Laser Ther. 16 (2) (2014) 96-103, https://doi.org/10.3109/14764172.2013.864198.
26. H.W. Choi, S.N. Abraham, In vitro and in vivo IgE-/Antigen-Mediated mast cell activation, Methods Mol Biol 1799 (2018) 71-80, https://doi.org/10.1007/978-1-4939-7896-0_7.
27. M.J. Monument, D.A. Hart, A.D. Befus, P.T. Salo, M. Zhang, K.A. Hildebrand, The mast cell stabilizer ketotifen fumarate lessens contracture severity and myofibroblast hyperplasia: A study of a rabbit model of posttraumatic joint contractures, J. Bone Joint Surg. Am. 92 (6) (2010) 1468-1477, https://doi.org/10.2106/JBJS.I.00684.
28. K.N. Kanada, T. Nakatsuji, R.L. Gallo, Doxycycline indirectly inhibits proteolytic activation of tryptic kallikrein-related peptidases and activation of cathelicidin, J. Invest. Dermatol. 132 (5) (2012) 1435-1442, https://doi.org/10.1038/jid.2012.14.
29. A. Di Nardo, A.D. Holmes, Y. Muto, E.Y. Huang, N. Preston, W.J. Winkelman, R.L. Gallo, Improved clinical outcome and biomarkers in adults with papulopustular rosacea treated with doxycycline modified-release capsules in a randomized trial, J. Am. Acad. Dermatol. 74 (6) (2016) 1086-1092, https://doi.org/10.1016/j.jaad.2016.01.023.
30. J.E. Choi, T. Werbel, Z. Wang, C.C. Wu, T.L. Yaksh, A. Di Nardo, Botulinum toxin blocks mast cells and prevents rosacea like inflammation, J. Dermatol. Sci. 93 (1) (2019) 58-64, https://doi.org/10.1016/j.jdermsci.2018.12.004.
31. M. Dyson, D.A. Luke, Induction of mast cell degranulation in skin by ultrasound, IEEE Trans Ultrason Ferroelectr Freq Control 33 (2) (1986) 194-201, https://doi.org/10.1109/t-uffc.1986.26814.
32. K. Aroni, E. Tsagroni, N. Kavantzas, E. Patsouris, E. Ioannidis, A study of the pathogenesis of Rosacea: How angiogenesis and mast cells may participate in a complex multifactorial process, Arch. Dermatol. Res. 300 (3) (2008) 125-131, https://doi.org/10.1007/s00403-007-0816-z.
33. V. Siqueira, M. Evangelista, S.A. Dos, R.L. Marcos, A.P. Ligeiro-De-Oliveira, C. Pavani, A.S. Damazo, A. Lino-Dos-Santos-Franco, Light-Emitting Diode treatment ameliorates allergic lung inflammation in

experimental model of asthma induced by ovalbumin, J. Biophotonics 10 (12) (2017) 1683-1693, https://doi.org/10.1002/jbio.201600247.

34. R. Kouhkheil, M. Fridoni, M.A. Abdollhifar, A. Amini, S. Bayat, S.K. Ghoreishi, S. Chien, M. Kazemi, M. Bayat, Impact of photobiomodulation and condition medium on mast cell counts, degranulation, and wound strength in infected skin wound healing of diabetic rats, Photobiomodul Photomed Laser Surg 37 (11) (2019) 706-714, https://doi.org/10.1089/photob.2019.4691.

Figures

Figure 1

Intense pulsed light (IPL) effectively alleviates rosacea

Clinical manifestation and red area images as analyzed by VISIA® before the treatment **(**Patient 1: **a1–a6,** patient 2: **c1–c6.)** and 1 month after IPL treatment **(**Patient 1: **b1–b6,** patient 2: **d1–d6)**; **(e)** ImageJ was used to determine the percentage of redness in VISIA images. **(f–g)** IGA and CEA scores before and after treatment. Statistical signifificance was assessed by Student's t-test (*** P < 0.001,* P < 0.05). Data is shown as mean ± SEM.

Figure 2

Intense pulsed light (IPL) treatment ameliorated rosacea-like inflammation and mast cell degranulation induced by LL-37 in mouse skin

(a) PBS or cathelicidin LL-37 (50μL, 320 μM) was injected intradermally into BALB/c mice to induce rosacea-like inflammation. Furthermore, two groups of mice were treated with IPL (IPL setting of 590-nm filter, single pulse with a 20-ms duration, and fluence of 11 J/cm^2) 12 h after the last injection, and animals were observed 1 h after IPL treatment. **(b–e)** Skin phenotype of different groups 1 h after the treatment: **(b)** Control group (only injected with PBS). **(c)** LL-37 group (only injected with LL-37); **(d)** LL-37+IPL group (injected with LL-37 and IPL treatment 12 h after the last injection). **(e)** IPL group (injected with 50 μL PBS and treated with IPL). **(f–i)** hematoxylin and eosin (H&E) staining of skin samples from the four groups reveals evident inflammation in the skin of the LL-37 group, which was significantly decreased in the LL-37+IPL group (Scale bar, 50 μm; n = 3). **(j–m)** MCs in the dermis were counted and in murine skin to assess the effect of IPL *in vivo*. Intact and degranulating MCs are indicated by a black arrow and white arrow, respectively. Toluidine blue staining of skin samples from the four groups reveals profound degranulated MCs were found in the skin of the LL-37 group **(k1–k2)** compared with the control group **(j1–j2)**, which was significantly decreased in the LL-37+IPL group (**l1–l2**), while the IPL group **(m1–**

m2) did not have evident changes (Scale bar, 50 μm; n = 10). **(n)** The value of “a” determined with a L*a*b colorimeter. **(o–p)** The proportion of MCs degranulation of mice under toluidine blue staining and MC counts per high magnification in each group. Statistical signifificance was assessed by one-way ANOVA (***P < 0:001,**P < 0:01, *P < 0.05).

Figure 3

Intense pulsed light (IPL) effectively suppressed the LL-37-induced increase in MMP-9, KLK5, cathelicidin, histamine, tryptase, and IL-6 expression in mouse skin

(a) Expression of MMP-9, KLK5, cathelicidin, histamine, tryptase and IL-6 was found to increase in the LL-37 group compared to that in the control group and decreased in the LL-37+IPL group (Scale bar, 50 μm; n ≥ 4). **(b–g)** Statistical signifificance was assessed by one-way ANOVA (***P < 0:001,**P < 0:01, *P < 0.05). Data is shown as mean ± SEM.

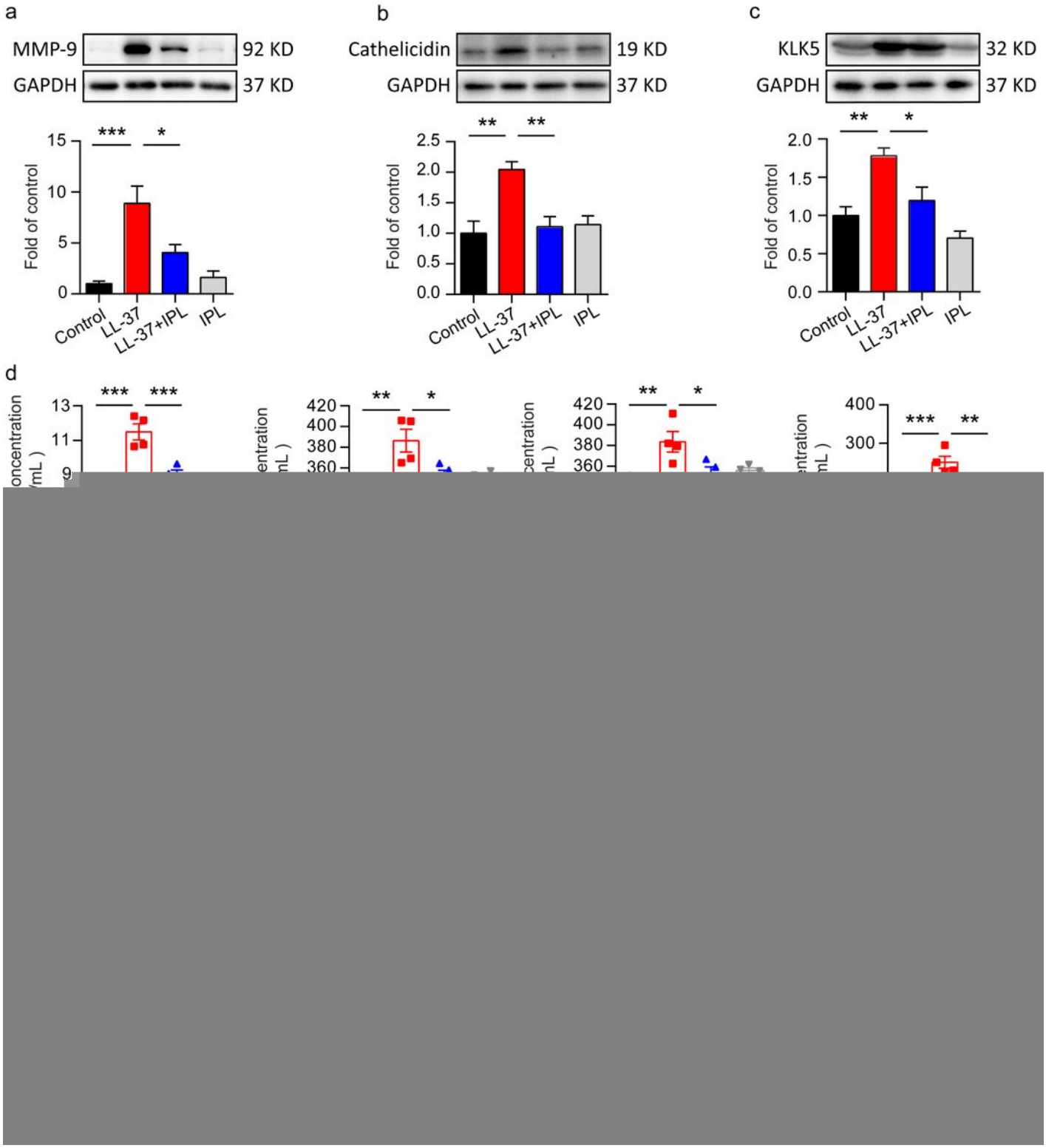

Figure 4

Intense pulsed light (IPL) treatment inhibited the expression of MMP-9, KLK5, and cathelicidin in a rosacea-like inflammation mouse model

(a–c) Western blot analysis and quantitative results of MMP-9, cathelicidin and KLK5 (n ≥ 4). **(d)** Statistical analysis results of ELISA for histamine, β-Hex, TNF-*α*, and IL-8. **(e)** Statistical analysis of the

qRT-PCR results of *Camp, Mmp9, Klk5, Cma1, Tpsab1, Cxcl2, Il1b, Il6* and *Tnf*a (n=4). Statistical significificance was assessed by one-way ANOVA (***P < 0:001, **P < 0:01, *P < 0.05). Data is shown as mean ± SEM.

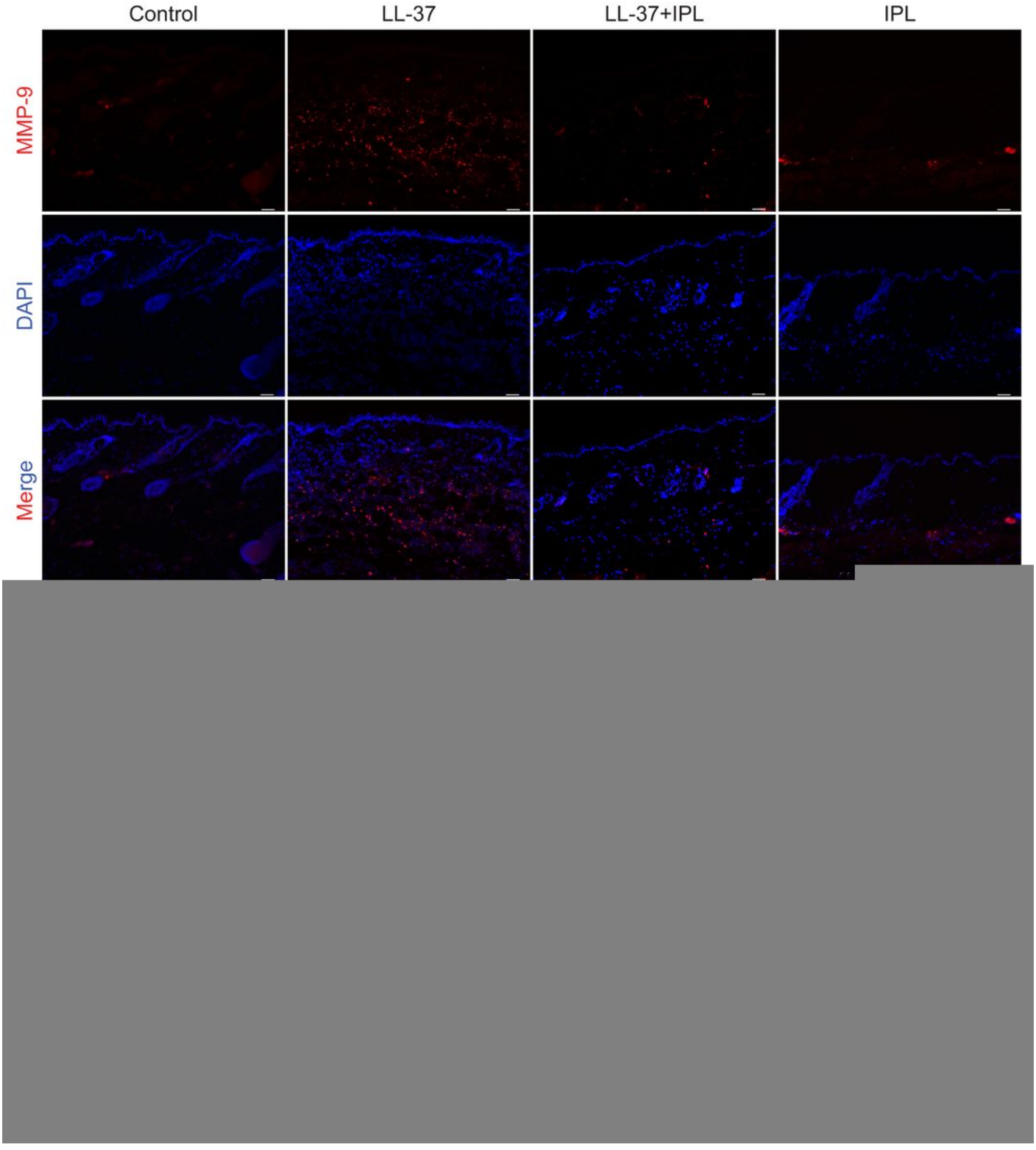

Figure 5

Intense pulsed light (IPL) treatment significantly suppressed the LL-37-induced increase in MMP-9 and KLK5 expression in mouse skin

MMP-9 and KLK5 expression following immunofluorescence detection in the skin tissues. Immunofluorescence staining of MMP-9 and KLK5 showed that IPL alleviated the LL-37 induced increase in expression of MMP-9 and KLK5, while only IPL did not cause any evident changes compared with the control. Pictures were taken under 200× magnification (Scale bar, 50 μm□n=3).

Figure 6

Intense pulsed light (IPL) alleviated the increased expression of MMP-9, KLK5, and cathelicidin in P815 mast cells induced by LL-37

The inflammatory model was established by a 6-hour exposure to LL-37 and then processed with or without IPL treatment. **(a)** Cell viability changed evidently with IPL with fluence ≥17 J/cm^2. **(b)** Cell viability decreased with LL-37 with a concentration ≥2.5 μM. **(c-f)** The increased expression of MMP-9, KLK5, and cathelicidin induced by LL-37 was alleviated by IPL. **(g)** Statistical difference was found between the secretion of mast cell (MC)-related proteases (histamine and β-Hex) and inflammatory factors (including TNF-a, IL-1β, and IL-8) between the LL-37 and the control groups, while also IPL could decrease the tendency, according to the ELISA results. **(h)** The gene expression of MC-related inflammation markers (*Tnfa*, *Il6*, and *Il8*) was also found to be greater in the LL-37 group than the control, which was also alleviated by IPL. Statistical signifificance was assessed by Student's t-test for **(a,b)** and one-way ANOVA test for **(d-h)** (***P < 0:001, **P < 0:01, *P < 0.05). Data is shown as mean ± SEM.

Supplementary Files

This is a list of supplementary files associated with this preprint. Click to download.

- Supplementarymaterial.pdf